Transmission line relay mis-operation detection based on time-synchronized field data

Article *in* Electric Power Systems Research · April 2015

DOI: 10.1016/j.epsr.2015.04.008

3 authors:

Ahad Esmaeilian
Texas A&M University

Tomo Popovic
University of Donja Gorica

Mladen Kezunovic
Texas A&M University

Electric Power Systems Research 125 (2015) 174–183

Contents lists available at ScienceDirect

Electric Power Systems Research

journal homepage: www.elsevier.com/locate/epsr

Transmission line relay mis-operation detection based on time-synchronized field data

Ahad Esmaeilian*, Tomo Popovic, Mladen Kezunovic

Department of Electrical and Computer Engineering Texas A&M University, College Station, TX, USA

ARTICLE INFO

Article history:
Received 20 January 2015
Received in revised form 10 April 2015
Accepted 11 April 2015

Keywords:
Fault detection
Fault location
Power system faults
Power system protection
Relay mis-operation
Time-synchronized measurements

ABSTRACT

In this paper, a real-time tool to detect transmission line relay mis-operation is implemented. The tool uses time-synchronized measurements obtained from both ends of the line during disturbances. The proposed fault analysis tool comes into the picture only after the protective device has operated and tripped the line. The proposed methodology is able not only to detect, classify, and locate transmission line faults, but also to accurately confirm whether the line was tripped due to a mis-operation of protective relays. The analysis report includes either detailed description of the fault type and location or detection of relay mis-operation. As such, it can be a source of very useful information to support the system restoration. The focus of the paper is on the implementation requirements that allow practical application of the methodology, which is illustrated using the field data obtained the real power system. Testing and validation is done using the field data recorded by digital fault recorders and protective relays. The test data included several hundreds of event records corresponding to both relay mis-operations and actual faults. The discussion of results addresses various challenges encountered during the implementation and validation of the presented methodology.

1. Introduction

Transmission line faults have to be confirmed and located quickly and accurately in order to restore power delivery as quickly as possible. Historical events show that most of the large scale blackouts occurred due to a series of transmission lines experiencing disturbances leading to relay mis-operations [1–3]. When a transmission line is tripped due to the operation of protective relays, an accurate fault analysis can verify whether the operation of relay was correct. Incorrect and unwanted relay trips of healthy lines are called relay mis-operations [4]. Distance relay mis-operation can happen due to incorrect first zone setting, false trip of the second zone, false trip of the third zone after a power swing in the network, etc. Moreover, in the case of fault, it can provide the operator with an accurate estimation of the fault location to facilitate the restoration process. The confirmation and isolation of the faulted sections by the operator, as well as evaluating the relay operation by protection engineer is also possible by utilizing such fault analysis tools [5]. There are several benefits of the use of automated fault data analytics such as increased reliability, personnel productivity, redundancy, all of which enhance timely support to the operations during the restoration or other critical decision making processes during disturbances [6]. Such analytic tools can also be very useful in support of reliable implementation of new applications such as transmission line switching (topology) control [7].

Different fault analysis methods have been proposed in the literature either as a separate fault detection, classification, and location functions or as a complete fault analysis tool [8–24]. A group of methods are developed, considering line impedance calculation [8–17], while several others are based on high-frequency transients, traveling waves, and wavelet-based methods [18–21]. Regardless of different schemes presented in these works, the advantages of high-frequency based methods are the high accuracy and fast decision making. However, the majority of these methods demand very high measurement sampling rate in the order of tens of kilohertz, which is still not extensively available in utilities.

In recent decades, several researchers developed an artificial neural network (ANN) and fuzzy logic-based algorithms to detect, classify and locate faults [22–24]. Generally speaking, the huge number of training sets needed to reflect the wide range of system operating conditions (i.e., loading condition, fault resistance, fault inception instance, etc.) makes these methods difficult to

* Corresponding author. Tel.: +1 979 862 1097; fax: +1 979 845 9887.
E-mail address: ahadesmaeilian@tamu.edu (A. Esmaeilian).

http://dx.doi.org/10.1016/j.epsr.2015.04.008
0378-7796/

implement in the industry environment. All of the methods described in the references above did not have a capability to detect or confirm relay mis-operations.

This paper presents an automated transmission line fault analysis that is able to detect, classify, locate faults, as well as to detect relay mis-operations. The method operates on measurements captured at both ends of the line tripped by protection relays. The purpose of the tool is to quickly confirm faults or detect relay mis-operations in order to expedite troubleshooting. Relay mis-operations detection can be very useful, especially if done within few minutes, in order to quickly mitigate the problem and prevent potential cascade. The method was validated using artificially simulated test cases and tested using actual fault and mis-operation data. The tool overcomes time response and accuracy shortcomings of the previous methods. The core algorithm is introduced in [25], and its practical implementation is demonstrated in this paper using real data captured in the field [26–30]. The paper first gives theoretical background, and then addresses requirements, challenges, and benefits related to the use of the proposed methodology.

2. Theoretical background

Researchers developed various fault analysis tools implemented with ambitions to be a complete package [31–33]. In [31,32], authors defined the algorithms based on availability of phasor measurements obtained from substation IEDs. As a result, the algorithms still needed phasor calculations which may decrease the speed and accuracy of methods. The approach presented in [33] is rather accurate but it depends on an availability of huge sets of training data and high sampling rate, which are not commonly available.

The fault analysis tool proposed in this paper, directly utilize time-synchronized sampled data recorded by event-triggered intelligent electronic devices (IEDs). The advantage of the proposed method over current differential based fault analysis methods proposed in literature is the direct use of samples without computing phasors, which reduces computational burden as well as the required available post fault data. Due to fast operations of digital relays and modern circuit breaker, the available post fault data window can be very short, which can hugely affect the accuracy of phasor based methods. It provides the operator and protection engineer with an accurate and detailed fault analysis report that includes information such as fault detection, fault type classification, internal/external fault differentiation, fault location estimate, or relay mis-operation indication. The primary goal of the presented method is to support decision making process when troubleshooting transmission line faults. The fault analysis core algorithm has been introduced in [25]. The following subsections provide an overview of fault detection, fault classification, and fault location calculation techniques implemented in the proposed solution.

2.1. Fault detection and classification scheme

The proposed method of fault detection and classification compares the change of direction of instantaneous powers at two ends of transmission line using synchronized sampling measurement. The method uses raw data measurements extracted from the data samples with no need for phasor calculations. The method was evaluated using both current differential and differential active power values. The use of active power displayed better accuracy as it was less affected by the presence of noise or higher frequencies in the current differential measurements.

In Fig. 1, $V_1(t)$, $I_1(t)$ and $V_2(t)$, $I_2(t)$ represent voltage and current measured at two ends (Bus 1 and Bus 2) of the line at instance t, respectively. Instantaneous powers can be calculated at both ends using following formulas:

$$P_1(t) = V_1(t) \times I_1(t) \tag{1}$$

$$P_2(t) = V_2(t) \times I_2(t) \tag{2}$$

The unique feature of instantaneous power measurements from both ends under fault condition makes the detection and classification of faults possible without using any thresholds. $P_1(t)$ and $P_2(t)$ phase angles are opposite to each other during the normal condition. However, during a fault, the faulty phases will be almost in phase with each other. It should be noted that, even after the fault inception, the phase opposition is maintained in phases that do not experience a faulted condition. Representing this feature mathematically can be done using a signum function defined as:

$$sgn(x) = \begin{cases} -1, & x < 0 \\ 0, & x = 0 \\ 1, & x > 0 \end{cases} \tag{3}$$

After calculation of sgn($P_1(t)$) and sgn($P_2(t)$), plotting the difference for each phase as Eq. (4) can give a clear understanding of how the algorithm differentiate between fault and normal condition.

$$Psgn(t) = sgn(P_1(t)) - sgn(P_2(t)) \quad \text{for} \quad \text{phase} \quad a, b, c \tag{4}$$

Theoretically, the sign difference introduced in Eq. (4) should be ± 2 before fault and during fault it should be 0; however, due to transients, noise, and bus angle differences, some outliers may be present. A moving time window of 5 ms is applied to the samples to check whether at least 90% of Psgn(t) are 0. The 90% threshold was used to allow for a certain level of outlier tolerance. This part of the algorithm has been enhanced by using a time window with variable length and thresholds, as it will be discussed in the implementation section.

Finally, if $P\text{sgn}(t) \approx 0$ for all phases, the fault type is a three phase fault, otherwise if $P\text{sgn}(t) \approx 0$ for two phases, then the fault is a double-phase fault. If $P\text{sgn}(t) \approx 0$ for only one phase, then the fault type is a single-phase-to-ground fault and otherwise there is no fault.

2.2. Fault location scheme

The concept of the fault location method utilized in the fault analysis tool was introduced in [34] and further developed in [25]. After detection of a faulty line, the fault location method is triggered utilizing fault type classification output to define the correct mode of the fault location calculation. Depending on the line length, two approaches have been developed to provide a better accuracy. For short transmission lines, only serial connection of an inductance and a resistance are taken into account. Kirchhoff voltage law from each end of the line to the fault point is applied assuming the line to be homogenous. After calculation and simplification, an explicit form of the fault location equation

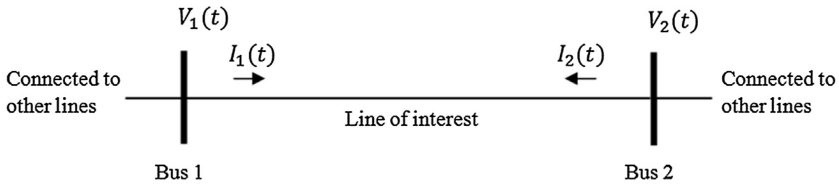

Fig. 1. Transmission line with two-end measurements.

is derived:

$$X_S=\frac{-\sum\limits_{m=a,b,c}\sum\limits_{k=1}^{N}A_m(k)B_m(k)}{\sum\limits_{m=a,b,c}\sum\limits_{k=1}^{N}B_m^2(k)}$$
$$A_m(k)=v_{mR}(k)-v_{mS}(k)-d\sum_{p=a,b,c}\begin{bmatrix}\left(R_{mp}+\left(L_{mp}/\Delta t\right)\right)i_{pR}(k)\\-\left(L_{mp}/\Delta t\right)i_{pR}(k-1)\end{bmatrix}$$
$$B_m(k)=d\sum_{p=a,b,c}\begin{bmatrix}\left(R_{mp}+\left(L_{mp}/\Delta t\right)\right)\left[i_{pR}(k)+i_{pS}(k)\right]\\-\left(L_{mp}/\Delta t\right)\left[i_{pR}(k-1)+i_{pS}(k-1)\right]\end{bmatrix}$$
$$m=a,b,c \tag{5}$$

where, subscripts S and R stand for the values at sending and receiving ends respectively. k is the present sample point; d is the per unit distance from S to fault point; Δt is the time period with respect to the sampling frequency;

Applying the same methodology for long transmission lines, represented using distributed parameters, resulted in a pair of recursive equations as below:

$$v_j(k)=\begin{bmatrix}\left(1/2\right)\left[v_{j-1}(k-1)+v_{j-1}(k+1)\right]\\+\left(Z_c/2\right)\left[i_{j-1}(k-1)-i_{j-1}(k+1)\right]\\+\left(R\Delta x/4\right)\left[i_{j-1}(k+1)-i_{j-1}(k-1)\right]\end{bmatrix} \tag{6}$$

$$i_j(k)=\begin{bmatrix}\left(1/2Z_c\right)\left[v_{j-1}(k-1)-v_{j-1}(k+1)\right]\\+\left(1/2\right)\left[i_{j-1}(k-1)+i_{j-1}(k+1)\right]-\left(R\Delta x/2Z_c\right)i_j(k)\\-\left(R\Delta x/4Z_c\right)\left[i_{j-1}(k-1)+i_{j-1}(k+1)\right]\end{bmatrix} \tag{7}$$

where, $\Delta x=\Delta t/\sqrt{LC}$ is the distance that the wave travels with a sampling time step Δt, $Z_c=\sqrt{L/C}$ is the surge impedance and subscript j is the position of the discretized point of the line.

The explicit form of fault location, equation cannot be derived from recursive voltage and current Eqs. (6) and (7). Therefore, following steps have been added to calculate the final location of fault.

Step 1. The line is discretized into equal segments with length of Δx.

Step 2. The approximate fault segment is calculated by finding the point that has the minimum square of voltage difference calculated from both ends. Since the line is assumed to be homogenous, the calculated voltage profile from both ends of the line must have the same value at fault point.

Step 3. Finally, a short line model is developed around the approximate fault point to refine the fault location using Eq. (5).

3. Implementation requirements

A typical transmission line setup with the event-triggered measurements from both ends is depicted in Fig. 2. As shown for Substation 1, the line can be monitored by various IEDs. For a single fault event, several IEDs can be triggered and produce event data files. The data samples are synchronized and time-stamped using a highly accurate time-reference clock signal generated by the Global Positioning System (GPS) receivers. The IED event files need to be efficiently communicated, grouped by events that triggered their creation, and paired base on their location (i.e., two ends of a transmission line).

The proposed implementation is illustrated with a diagram in Fig. 3. The implementation assumes a high-speed communication link between substations and control center in order to reduce download time from DFR/DPR devices. The analysis reports need to be stored in a central database and made accessible to the operator and protections engineers. Details on the implementation requirements and challenges pertinent to the use of field data are discussed in the following subsections.

3.1. Importing the event data

DFR/DPR event files were received from the participating utility in unified COMTRADE file format (IEEE C37.111-1999). The used DFR and DPR devices varied by vendor, types, and vintage. The field data measurements varied in sampling frequency, vertical A/D resolution, accuracy in time synchronization, etc. The sampling rate was 96 samples per cycle for DFRs and 16 samples per cycle for DPRs.

The system model description was received in PSS/E raw file format and used for pairing the event files coming from two ends of the same transmission line. Finally, the utility provided a spreadsheet containing the list of relay mis-operations and references to the corresponding event files.

3.2. Pairing the two-end data

The correct operation of the method requires measurements from both ends of the line with the correct time reference. If there is only a file from one end of the line, it is kept in the event database to be used if the data from remote buses becomes available. As mentioned before, there can be multiple IED files created during a single disturbance event. The files corresponding to the same event can be identified using the GPS time stamp. Furthermore, using the topology from the system model, the IED files from the neighboring nodes are paired to extract the two-end measurement for the transmission line between the nodes (buses). The following steps are needed to pair the two-end data:

Step 1. Extraction of substation name from the currently processed event file name (assuming the use of IEEEC37.232-2011 naming convention).

Step 2. By utilizing static system model from PSS/E file, a topology processing script identifies all possible neighboring nodes with respect to node currently being processed.

Step 3. The file repository is checked to focus on the nodes for which the event data exist.

The analysis is then performed for each available pair of data files.

One of the challenges experienced with the field data was a lack of substation naming convention, which resulted in a

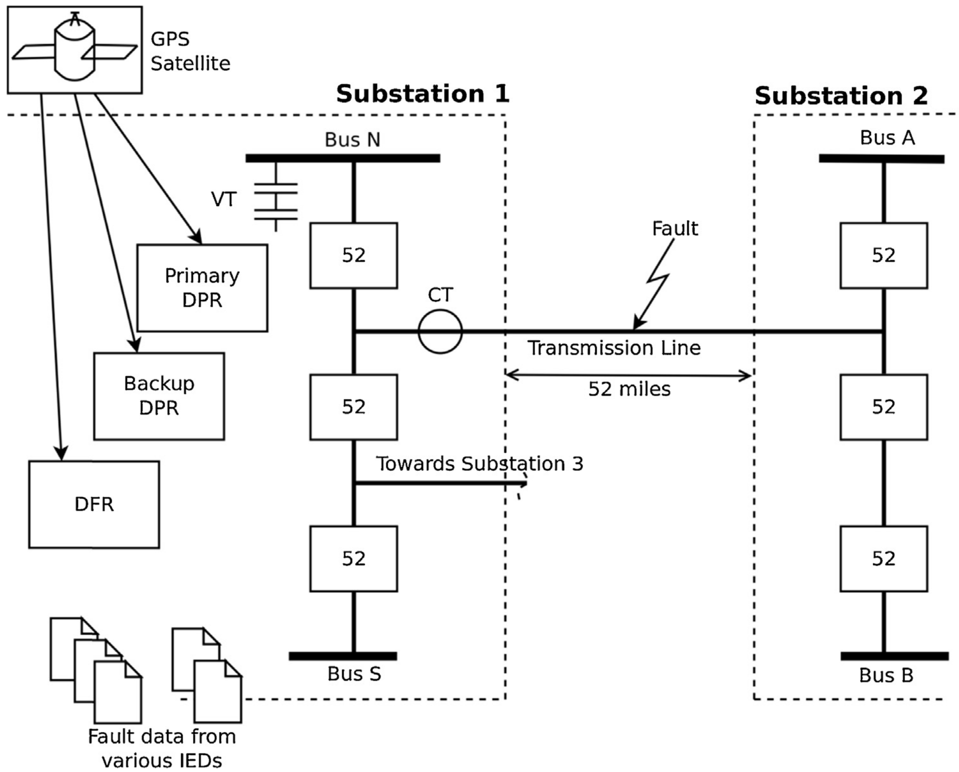

Fig. 2. Typical transmission line setup with measurements from both ends.

mismatch between information the PSS/E file vs. channel names in DFR/DPR files. A considerable portion of the DFR/DPR files could not be matched automatically and these files had to be checked manually to extract all possible test cases.

3.3. *Re-sample and align*

Most modern IEDs support synchronous sampling using the information obtained from a GPS receiver. Files corresponding to two-end measurements of the same event are processed in order to extract data samples for instantaneous voltage and current signals measured at both ends of the line. The extracted data samples are re-sampled and aligned to allow for algorithms that use instantaneous values to be applied. Re-sampling is done using interpolation in order to obtain the same sampling rate for measurements collected at both ends. The alignment of the event records is done to compensate for the different lengths of pre-disturbance data windows for different IEDs, which is a common situation. Fig. 4 shows an example of a situation where recordings of the same event had a difference in the pre-fault duration. As it can be seen, the pre-fault time captured by DFRs at ends 1 and 2 are 85 ms and 253 ms, respectively.

The final result of the signal processing is a set of synchronized samples corresponding to phase voltage and current signals from both ends of the transmission line in question.

3.4. *Fault analysis*

In [25], a single length moving window of 5 ms was used with the threshold set at 90%, since the software simulated data were relatively clean of higher frequency, noises, and other corrupting factors. The actual implementation uses a variable length time moving window (5, 10, and 15 ms lengths) to check whether at least 80% (this threshold value was determined considering a certain level of outliner) of $Psgn(t)$ are 0. A sensitivity study using the available field data was performed to determine thresholds to be used with each time-window size. The modified algorithm performs a three-step check:

Step 1. First, the algorithm checks the possibility of fault with a 5 ms window and 90% threshold;

Step 2. If no fault is detected, a 10 ms window with 85% threshold is used;

Step 3. Finally, a time window of 15 ms with 80% threshold value will be applied, accordingly. If the fault is not detected, the event is considered a relay mis-operation.

3.5. *Detailed report*

The results of fault analysis are provided in the form of detailed analysis report. As shown in Fig. 3, the outcome of the analysis may be: (a) the event is not a fault, which means that the tripped line may be available to switch back in; (b) fault detected, classified, and

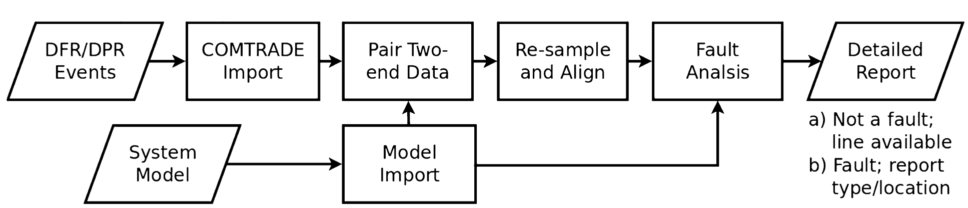

Fig. 3. Automated analysis of time-synchronized event data.

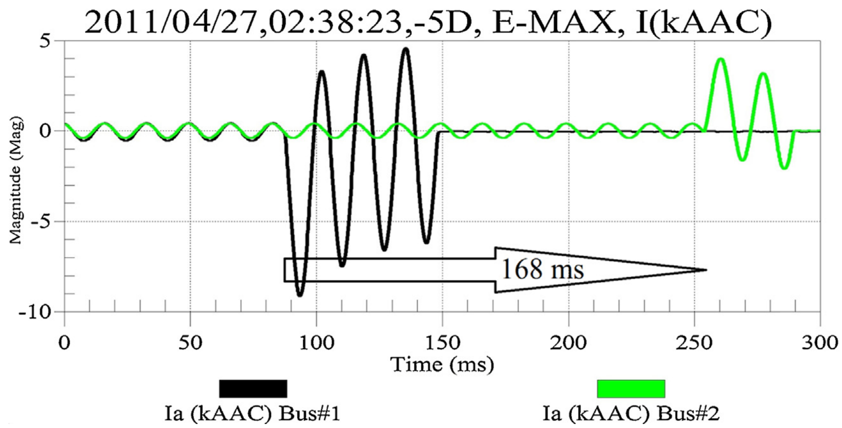

Fig. 4. DFR extracted current waveforms before time synchronization.

the distance to fault has been estimated. During the evaluation, the analysis results were compared with the actual scenarios to assess the errors. The results were saved for further studies.

3.6. Data analytics execution sequence

The execution process for the analysis tool and its main components is illustrated with a sequence diagram in Fig. 5. The initialization of the tool reads the settings (i.e., incoming data folder, channel assignments) and the system topology given in PSS/E raw file format. The main module continuously scans the incoming folder and once a new event file is detected, it is imported into the event database. For the given source bus where the file was recorded, the analysis checks the system topology to identify all the remote substations (neighboring buses). The event database is then queried for all the available data files from remote buses that were recorded at the similar time (time window set at 100 ms). If the two-end paired data is found, i.e., there are at least two event records corresponding to the same event, the fault analysis is applied. The analysis is repeated for each line with two-end fault data as depicted in Fig. 5. An analysis report is generated for each processed pair of two-end data and archived in the database for later use. The total time budget for the execution is measured in minutes (i.e., <5 min). Most of the time is used to transfer event files from substation IEDs to the centralized workstation.

4. Validation using simulated data

The proposed analytic tool has been validated using simulated fault data. The IEEE 118 bus test system has been simulated in ATP software [35]. A MATLAB script has been developed to create large number of test cases in ATP software [36]. Table 1 illustrates a

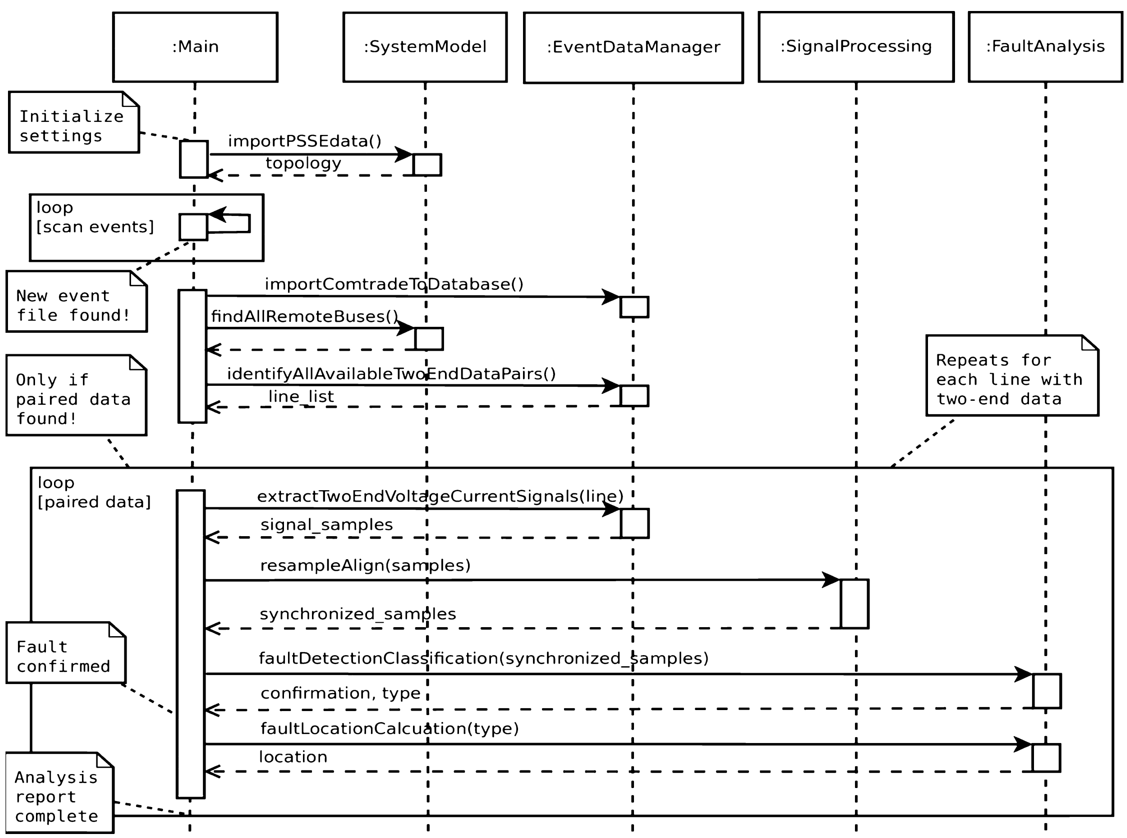

Fig. 5. Sequence diagram of the relay mis-operation detection software.

Table 1
Summary of result of ATP simulations.

Fault specification			Sampling frequency					
Fault type	Fault resistance (Ω)	Fault distance (%)	500 Hz		2 kHz		10 kHz	
			Fault location error (%)	Detected fault type	Fault location error (%)	Detected fault type	Fault location error (%)	Detected fault type
AG	1	5	1.74	AG	1.42	AG	1.04	AG
		20	1.53	AG	1.25	AG	0.81	AG
		50	0.35	AG	0.08	AG	0.15	AG
	10	5	2.16	AG	1.74	AG	1.18	AG
		20	1.97	AG	1.50	AG	0.93	AG
		50	0.52	AG	0.17	AG	0.21	AG
	100	5	2.31	AG	1.91	AG	1.48	AG
		20	2.16	AG	1.69	AG	1.25	AG
		50	0.79	AG	0.55	AG	0.23	AG
AB	1	5	1.86	AB	1.52	AB	1.15	AB
		20	1.63	AB	1.39	AB	0.92	AB
		50	0.41	AB	0.19	AB	0.15	AB
	10	5	2.33	AB	1.81	AB	1.26	AB
		20	2.01	AB	1.65	AB	0.99	AB
		50	0.75	AB	0.30	AB	0.20	AB
	100	5	2.57	AB	2.03	AB	1.41	AB
		20	2.28	AB	1.75	AB	1.12	AB
		50	0.83	AB	0.68	AB	0.04	AB
ABG	1	5	1.64	ABG	1.36	ABG	1.08	ABG
		20	1.49	ABG	1.17	ABG	0.80	ABG
		50	0.52	ABG	0.33	ABG	0.34	ABG
	10	5	1.95	ABG	1.52	ABG	1.02	ABG
		20	1.70	ABG	1.37	ABG	0.94	ABG
		50	0.42	ABG	0.29	ABG	0.17	ABG
	100	5	2.17	ABG	1.83	ABG	1.59	ABG
		20	1.92	ABG	1.62	ABG	1.30	ABG
		50	0.60	ABG	0.51	ABG	0.23	ABG
ABCG	1	5	1.51	ABCG	1.37	ABCG	0.95	ABCG
		20	1.33	ABCG	1.14	ABCG	0.79	ABCG
		50	0.19	ABCG	0.05	ABCG	0.07	ABCG
	10	5	1.77	ABCG	1.56	ABCG	1.15	ABCG
		20	1.58	ABCG	1.33	ABCG	0.93	ABCG
		50	0.26	ABCG	0.18	ABCG	0.11	ABCG
	100	5	1.94	ABCG	1.69	ABCG	1.04	ABCG
		20	1.78	ABCG	1.41	ABCG	0.88	ABCG
		50	0.41	ABCG	0.25	ABCG	0.15	ABCG

portion of validation results considering different fault specifications. As shown in Table 1, different fault types (AG, AB, ABG, ABCG), fault distances (5%, 20%, 50%), fault resistances (1 Ω, 10 Ω, and 100 Ω) and different sampling rates (500 Hz, 2 kHz, 100 kHz) were simulated. For all 108 cases, the fault has been correctly detected and classified. The results of fault location showed high accuracy (the worst case error is less than 2.5%) of the method even under very high fault resistances. Three observations were made during the validation testing: (a) as the sampling rate increases, the fault location error goes down for the same fault specification; (b) the result of fault location is more accurate when the fault occurs close to the middle of the line, which was expected for two-end algorithms; (c) the result of fault location is robust for both grounded and ungrounded systems.

5. Test results using field data

A description of the field data used for the implementation and validation of the new fault analysis tool is summarized in Table 2. The utility provided us with 1764 event files that have been collected from various substations over the period of 5 years. All of the events were caused by distance relays operation which occurred at the transmission level. As expected, a huge portion of the received event files were covering measurements from only one end of the line. After sorting the data and verifying the configuration availability, the total number of events for which there was a useful pair of two-end data was 181, which is still a representative set of field data test cases.

5.1. Examples of transmission line faults

Fig. 6(a–c) depicts instantaneous power $P_1(t)$ and $P_2(t)$ captured by DFR units at the two ends of a 161 kV transmission line with respect to time. In this case, the original information received from utility shows that the transmission line between two substations experienced a fault and relays at both ends tripped in first zone. The results of simulations show that fault detection and classification method detects a single phase fault (ag).

As shown in Fig. 6(a–c), the disturbance has started at 60 ms and the instantaneous powers from two ends at phase B and C are in the opposite direction before and after disturbance. While for phase A, they become in the same direction when the disturbance has been initiated. As a result, the output of the fault analysis tool reports “Single phase A to ground fault” condition. Fig. 7(d–f) shows plot of $P\mathrm{sgn}(t)$ with respect to the time for three phases. It is obvious that for phases B and C less than 80% of the total samples are zero while for phase A more than 80% of the total samples are zero.

Table 2
Summary of DFR/DPR Files Event Extraction.

Files availibility	IED device type (number of files)	Event type (number of files)	Total useful events
Multiple ends	DFR (450)/DPR (45)	Fault (106)/mis-operation (45)	151
Two ends	DFR (71)/DPR (17)	Fault (15)/Mis-Operation (15)	30
Single end	DFR (1083)/DPR (98)	Fault (375)/Mis-Operation (156)	0
Total	DFR (1604)/DPR (160)	Fault (496)/mis-operation (216)	181

5.2. *Examples of relay mis-operations*

Sometimes, distance relays trip in response to power swings phenomena, overload or occurrence of faults on adjacent transmission lines. In such cases, a fast corrective action to identify the relay mis-operation and switch the healthy line back to service may prevent power system from cascading outages and major blackouts. Fig. 7(a–c) depicts instantaneous power $P_1(t)$ and $P_2(t)$ calculated based on data captured by DFR units at the two ends of a 161 kV transmission line with respect to time. In this case, the initial information received by utility shows that the line has been falsely tripped due to single phase fault (ag) while the later investigation of the case reveals that the relay mis-operates due to a single phase fault on an adjacent line.

As it can be seen from Fig. 7(a–c), the disturbance has been started at 160 ms and the instantaneous powers from two ends are in the opposite direction before and after disturbance. As a result, the output of the fault analysis tool reports “no fault” condition. Fig. 8(d–f) shows plot of $P\mathrm{sgn}(t)$ with respect to time for three phases. It is obvious that less than 80% of the total samples are zero which means no fault has been detected in any of three phases.

In all of the received field test cases, the lines have been switched out due to operation of distance relays at both ends. The method would not be affected if only a relay at one end mis-operates. In such

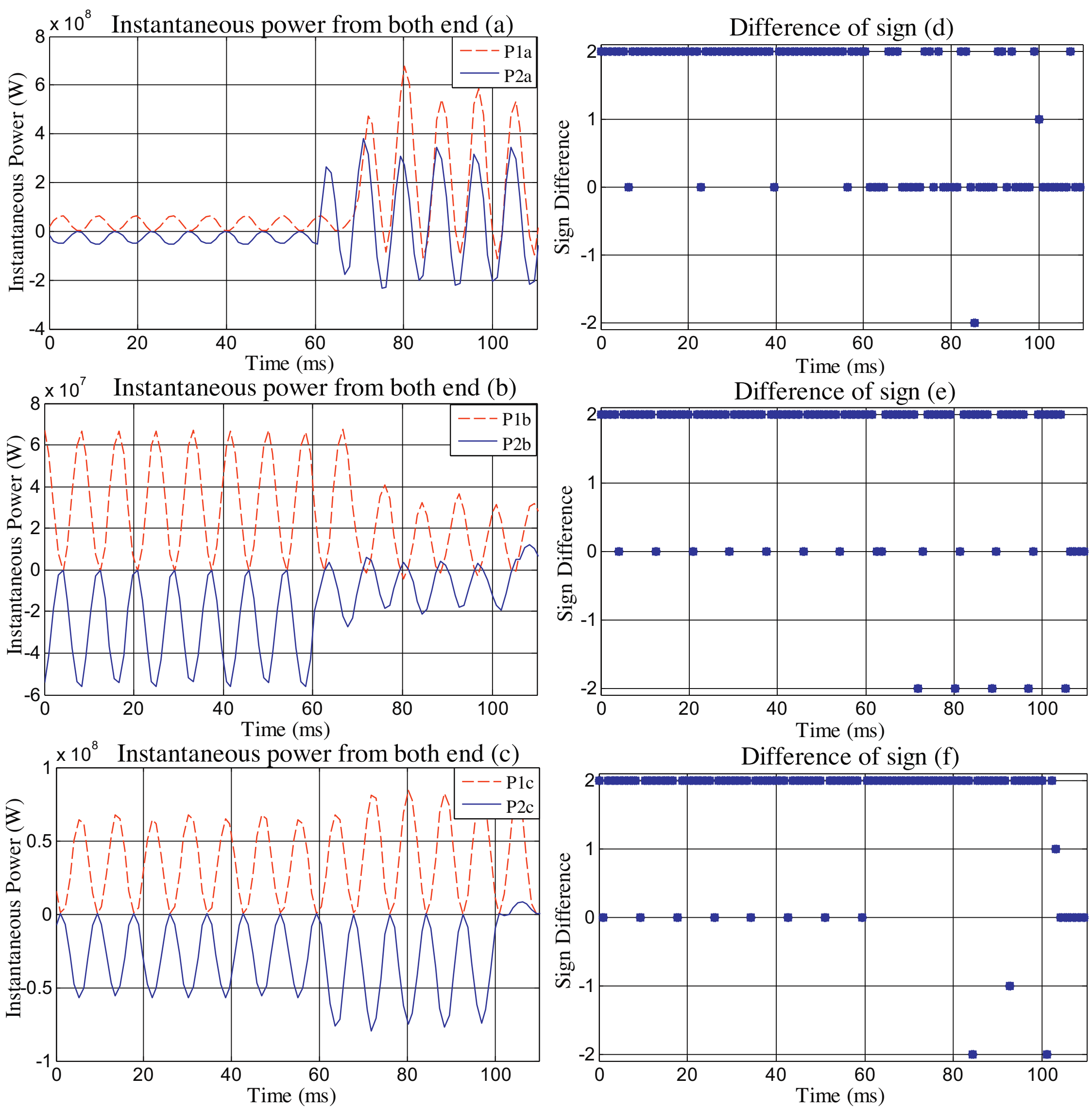

Fig. 6. Single phase to ground fault detection and classification.

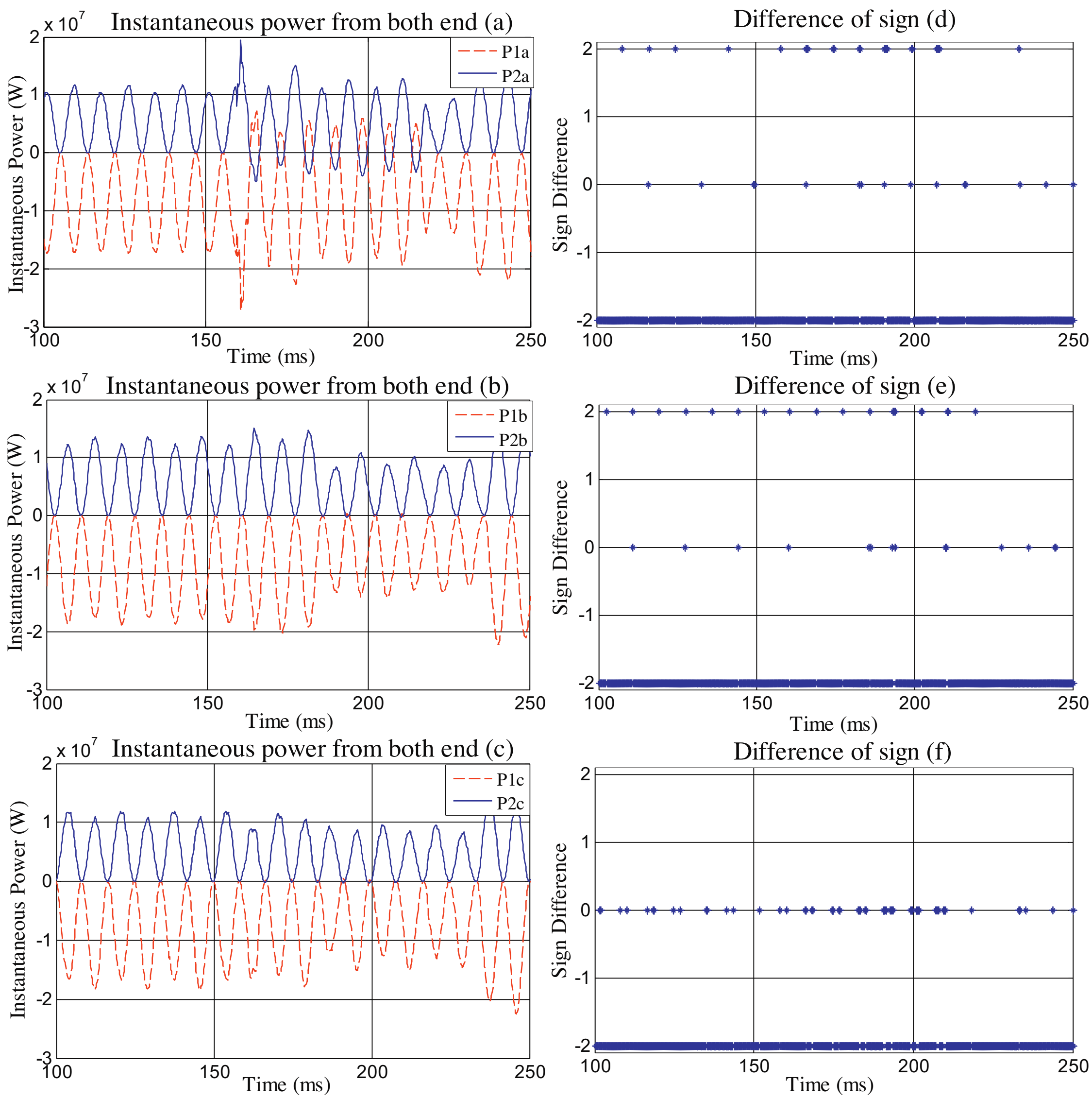

Fig. 7. Relay mis-operation detection.

cases, assuming that the DFR event files are available from both ends, the analysis would identify the line as being healthy and the relay mis-operation would be reported so that the operators and protection engineers can initiate mitigation or troubleshooting.

5.3. Additional two-end data analysis results

Table 3 provides a summary of the results for 10 fault and 10 relay mis-operation cases. As described in the theoretical background, the proposed method detects and classifies fault using the three step variable time length data window. In all cases, the algorithm detects, classifies and locates the faults within one cycle of fault inception, which reveals the speed of the tool. Utilizing this feature, we were able to achieve correct results even in the cases with short post fault data (due to fast operation of circuit breakers). The approach accurately and reliably detects relay mis-operation cases, which can be used as a source of information for corrective switching actions.

In many test cases, captured voltage and current signals were noisy and there was a concern that the noise will affect the analytics. For example, in Fig. 8 the waveforms are moderately affected by higher frequency noise. In the provided set of files, the fault analysis accurately detected faults and relay mis-operations even for the noisy signals. Future research should include a sensitivity study to determine effects of the noise to the analytic results.

5.4. Data from multiple ends

In this subsection, a unique feature of the fault analysis tool has been tested and verified. Theoretically, this fault analysis tool is able to operate when the DFR/DPR measurements are available at two ends of a line. The fault analysis tool can also be utilized when there are files from multiple ends. In such cases, the algorithm can detect the fault if it occurred inside any sets of two ends data.

Fig. 9 shows the topology of a part of a power system where multiple DFR data are captured when an event occurred. In this case, the DFR data are available at three specified buses while there are some buses in between where no DFR file is available. The fault analysis tool has been deployed for three different sets of two end data identified as route 1 to 3 in Fig. 9. To have a better insight in the fault analysis tool behavior, the ratio of zero samples to the total samples inside the moving window has been plotted against the time. Anytime the output exceeds 0.8 for any phase, it means a fault has been detected on such phase.

Table 3
Fault Analysis Tool Test Results vs. Field Data.

Test data category	Case number	kV level	Event type detected	Detection time (ms)	Fault location (pu)
Fault cases	1	161	ABG fault	5.1	0.071
	2	500	CG fault	7.9	0.514
	3	500	CG fault	9.2	0.463
	4	161	CG fault	5.8	0.817
	5	161	BG fault	8.7	0.789
	6	161	ACG fault	7.1	0.306
	7	161	AG fault	10.3	0.449
	8	161	BG fault	14.9	0.275
	9	161	AG fault	11.7	0.650
	10	161	AG fault	9.4	0.119
Relay mis-operation cases	1	161	Mis-operation	8.6	N/A
	2	161	Mis-operation	12.4	N/A
	3	500	Mis-operation	11.8	N/A
	4	161	Mis-operation	9.6	N/A
	5	161	Mis-operation	8.7	N/A
	6	161	Mis-operation	10.4	N/A
	7	161	Mis-operation	14.3	N/A
	8	161	Mis-operation	10.8	N/A
	9	161	Mis-operation	7.5	N/A
	10	161	Mis-operation	8.8	N/A

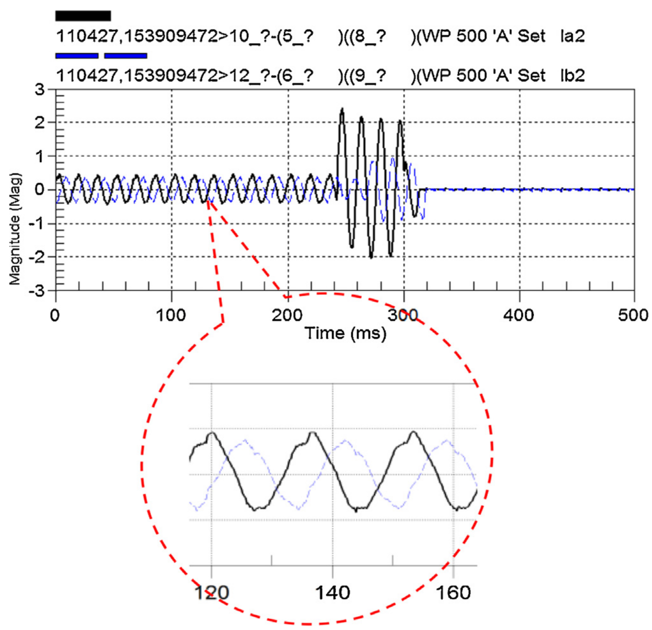

Fig. 8. Higher order harmonics and noise presence in current signals.

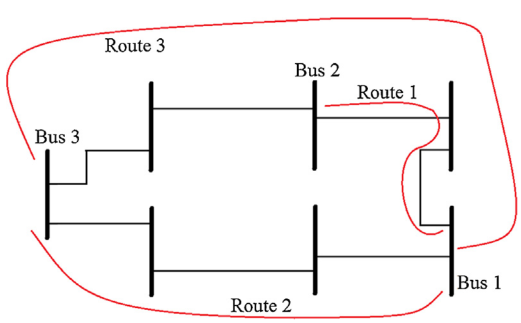

Fig. 9. System topology for multiple-end data.

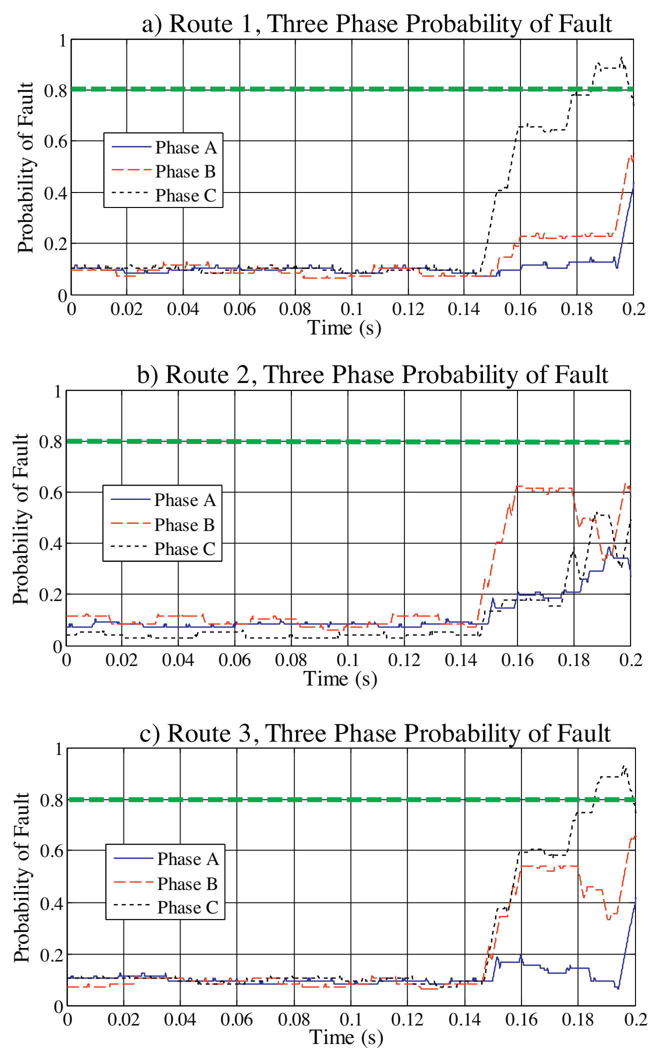

Fig. 10. Probability of the fault for the case of multiple-end data.

Fig. 10(a–c) depicts the outputs of the fault analysis tool for the three different routes described in Fig. 9. The results illustrate that a single phase A to ground fault is detected on route 1 and 3 while no fault has been detected on route 2. Using the pair of data from buses 1 and 2 the fault has been located at 0.56 pu from bus 1, while using the pair of data from bus 1 and 3, 0.63 pu from bus 1.

6. Conclusions

The main contributions of this paper are:

- It defines implementation requirements for the practical fault analysis solution for detection of relay mis-operations. Such a tool can be very useful to support decision making process during the system restoration and for prevention of cascading events.
- The implementation addressed the challenges pertained to the use of field data such as quality of field signals, time synchronization, different sampling rates and A/D resolutions, etc.
- The validation of the method was done using ATP simulations of IEEE 118 test system. The simulation included several test cases based on different fault type, fault resistance, distance to fault, sampling rates, etc.
- Finally, the implementation was tested using the actual field data, which included around 200 test cases. The correct operation has been validated against the information about the events received from the participating utility.

References

[1] M. Johnson, Line Protection and Power System Collapse (Master's Thesis), Department of Electric Power Engineering, Chalmers University of Technology, Goteborg, Sweden, 2001.

[2] "Final Report on the August 14, 2003 Blackout in the United States and Canada: Causes and Recommendations," U.S.-Canada Power System Outage Task Force, April 5, 2004.

[3] R. Baldick, B. Chowdhury, I. Dobson, D. Zhaoyang, G. Bei, D. Hawkins, et al., Initial review of methods for cascading failure analysis in electric power transmission systems, in: Proceedings of the IEEE PES General Meeting, Pittsburgh, PA, USA, Jul, 2008.

[4] M. Kezunovic, S. Meliopoulos, V. Venkatasubramanian, V. Vittal, Application of Time-Synchronized Measurements in Power System Transmission Networks, Springer, New York, 2014, pp. 152–159.

[5] M. Kezunovic, B. Perunicic, Automated transmission line fault analysis using synchronized sampling at two ends, IEEE Trans. Power Syst. 11 (1 (Feb)) (1996) 441–447.

[6] T. Popovic, M. Kezunovic, Measures of value: data analytics for automated fault analysis, IEEE Power Energy Mag. 10 (5 (Sept)) (2012) 58–69.

[7] M. Kezunovic, T. Popovic, G. Gurrala, P. Dehghanian, A. Esmaeilian, M. Tasdighi, Reliable implementation of robust adaptive topology control, in: Proceedings of the HICCS—Hawaii International Conference on System Science, Manoa, Hawaii, January, 2014.

[8] A. Ghaderi, H.A. Mohammadpour, H. Ginn, Active fault location in distribution network using time-frequency reflectometry, Power and Energy Conference at Illinois, Feb 2015, pp. 1–7.

[9] A. Ghaderi, H.A. Mohammadpour, H. Ginn, High impedance fault detection in distribution network using time-frequency based algorithm, IEEE Trans. Power Deliv. PP (99 (Oct)) (2014) 1–9.

[10] A. Ghaderi, A. Esmaeilian, M. Kalantar, A novel islanding detection method for constant current inverter based distributed generations, 10th International Conference on Environment and Electrical Engineering (EEEIC), May 2011, pp. 1–4.

[11] A. Esmaeilian, M. Mohseninezhad, M. Doostizadeh, M. Khanabadi, A precise PMU based fault location method for multi terminal transmission line using voltage and current measurement, 10th International Conference on Environment and Electrical Engineering (EEEIC), May 2011, pp. 1–4.

[12] P.-C. Chen, V. Malbasa, Y. Dong, M. Kezunovic, Sensitivity analysis of voltage sag based fault location algorithm, in: Proceeding of the 18th Power Systems Computation Conference (PSCC), Worclaw, Poland, 2014.

[13] P.-C. Chen, V. Malbasa, M. Kezunovic, Locating sub-cycle faults in distribution network applying half-cycle DFT method, IEEE PES 2014 T&D Conference and Exposition, Apr. 2014, pp. 1–5.

[14] P.-C. Chen, V. Malbasa, M. Kezunovic, Sensitivity of voltage sag based fault location in distribution network to sub-cycle faults, North American Power Symposium (NAPS), Sep. 2014.

[15] Y. Liao, Fault location for single-circuit line based on bus-impedance matrix utilizing voltage measurements, IEEE Trans. Power Deliv. 23 (2 (Apr)) (2011) 609–617.

[16] N. Kang, Y. Liao, Double-circuit transmission-line fault location with the availability of limited voltage measurements, IEEE Trans. Power Deliv. 27 (1 (Apr)) (2011) 325–336.

[17] A. Esmaeilian, M. Kezunovic, An Impedance Based Fault Location Algorithm For Tapped Lines Using Local Measurements, The 45th North American Power Symposium (NAPS), USA, Sep. 2013.

[18] C.Y. Evrenosoglu, A. Abur, Travelling wave based fault location for teed circuits, IEEE Trans. Power Deliv. 20 (2 (Apr)) (2005) 1115–1121.

[19] M. Korkali, H. Lev-Ari, A. Abur, Traveling-wave-based fault-location technique for transmission grids via wide-area synchronized voltage measurements, IEEE Trans. Power Deliv. 27 (2 (May)) (2012) 1003–1011.

[20] A.T. Johns, R.K. Aggarwal, Z.Q. Bo, A novel non-unit protection technique for EHV transmission systems based on fault-generated noise. Part 1. Signal measurement, IEE Proc. Gener. Trans. Distrib. 141 (2) (1994) 133–140.

[21] R.K. Aggarwal, A.T. Johns, Z.Q. Bo, A novel non-unit protection technique for EHV transmission systems based on fault-generated noise. Part 2. Signal processing, IEE Proc. Gener. Trans. Distrib. 141 (2) (1994) 141–147.

[22] M. Sanaye-Pasand, P. Jafarian, An adaptive decision logic to enhance distance protection of transmission lines, IEEE Trans. Power Deliv. 26 (4 (Oct)) (2011) 2134–2144.

[23] C. Pang and M. Kezunovic, Detection tools for disturbances and protective relay operations leading to cascading events, IEEE PES General Meeting, Calgary, Canada, Jul 2009.

[24] T.S. Sidhu, H. Singh, M.S. Sachdev, Design, implementation and testing of an artificial neural network based fault direction discriminator for protecting transmission lines, IEEE Trans. Power Deliv. 10 (2 (Apr)) (1995) 697–706.

[25] P. Dutta, A. Esmaeilian, M. Kezunovic, Transmission-line fault analysis using synchronized sampling, IEEE Trans. Power Deliv. 29 (2 (Apr)) (2014).

[26] S. Santoso, A. Gaikwad and M. Patel, Impedance-based fault location in transmission networks: theory and application.

[27] A. Gomes, M. Costa, T. de Faria, W. Caminhas, Detection and classification of faults in power transmission lines using functional analysis and computational intelligence, IEEE Trans. Power Deliv. 28 (3 (Jul)) (2013) 1402–1413.

[28] M. Sanaye-Pasand, O.P. Malik, High speed transmission line directional protection evaluation using field data, IEEE Trans. Power Deliv. 14 (3 (Jul)) (1999) 851–856.

[29] M.M. Eissa, Development and investigation of a new high-speed directional relay using field data, IEEE Trans. Power Deliv. 23 (3 (Jul)) (2008) 1302–1309.

[30] T. Popovic, M. Kezunovic, B. Krstajic, Implementation requirements for automated fault data analytics in power systems, Int. Trans. Electric. Energy Syst. 25 (4 (Apr)) (2015) 731–752.

[31] J.-Z. Yang, et al., An adaptive PMU based fault detection/location technique for transmission lines. I. Theory and algorithms, IEEE Trans. Power Deliv. 15 (2 (Apr)) (2000) 486–493.

[32] Y.-H. Lin, C.-W. Liu, C.-S. Chen, A new PMU based fault detection/location technique for transmission lines with consideration of arcing fault discrimination-part I: theory and algorithms, IEEE Trans. Power Deliv. 19 (4 (Oct)) (2004) 1587–1593.

[33] N. Zhang, M. Kezunovic, A real time fault analysis tool for monitoring operation of transmission line protective relay, Electr. Power Syst. Res. J. 77 (3–4 (Mar)) (2007) 361–370.

[34] A. Gopalakrishnan, M. Kezunovic, S.M. McKenna, D.M. Hamai, Fault location using distributed parameter transmission line model, IEEE Trans. Power Deliv. 15 (4 (Oct)) (2000) 1169–1174.

[35] EMTP, Alternative transients program. ⟨http://www.emtp.org/⟩, Dec. 2010.

[36] A. Abdullah, A. Esmaeilian, G. Gurrala, P. Dutta, T. Popovic, M. Kezunovic, Test Bed For Cascading Failure Scenarios Evaluation, IPST, Vancouver, Canada, 2013 (Jul).